

FR Dichotomy, Accretion Modes and Environmental Factors in the Local Universe

Melanie Gendre (JBCA), Philip Best (IfA Edinburgh) & Jasper Wall (UBC)

ABSTRACT

Active galactic nuclei (AGN) comprise the majority of currently observed radio galaxies, and the Fanaroff-Riley (FR) categorisation provides a classification of extended AGN. The FRI objects have the highest surface brightness along the jets near the core, while FR II sources show the highest surface brightness at the lobe extremities, as well as more collimated jets. This FR dichotomy is based purely on the appearance of the radio objects, and the mechanisms differentiating the two populations are still unknown. Two main streams of models exist to explain these differences in morphology. Extrinsic models are purely based on the source environment, where inter-galactic medium density is the differentiating factor: jets of sources in higher/lower density mediums experience a higher/lower degree of resistance, yielding sources with FRI/FR II structures respectively. Intrinsic models, on the other hand, suggest that the dichotomy arises from differences in the properties of the central black hole. In these scenarios, low-excitation galaxies (LEG) have jets produced by low accretion-flow rate which are generally weak and mostly display FRI-type structure, whereas high-excitation galaxies (HEG) have higher accretion flow rates giving rise to stronger, mainly FR II-type jets. If the FR dichotomy was fully dependent on the jet properties, FRI/II sources would be systematically associated with LEG/HEG respectively. However, in several cases, small subsets of FRIs were found in HEG samples, as well as some FR IIs being associated with LEGs.

CoNFIG LOCAL SAMPLE

In previous studies of FR sources using the CoNFIG catalogue (Gendre et al. 2008, 2010), results have shown that, at comparable powers, FRI and FR II sources show strong similarities in evolution, which indicate that they very probably share a common mechanism governing the luminosity-dependent evolution. In addition, radio luminosity function (RLF) models hint at a luminosity-dependent bimodal evolution, where low-luminosity sources show no evolution while high-luminosity sources undergo positive density evolution. What differentiates FR sources? Two main streams of models exist to explain these differences in morphology: Extrinsic models, purely based on the source environment (e.g. Prestage & Peacock 1988) and intrinsic models, suggesting that the dichotomy arises from differences in the properties of the central black hole (e.g. Ghisellini & Celotti 2001).

To test these scenarios, high/low excitation classification and environmental richness factor of a sub-sample of local ($z \leq 0.3$) CoNFIG extended galaxies were compiled to investigate the possible FR morphology/accretion mode/environment relations. The sub-sample contains 206 sources, including 74 FRIs and 107 FR IIs, 76% of which have available spectra, mostly from SDSS.

CLUSTER RICHNESS

Cluster richness was determined using the method of Wing & Blanton (2011), in which the richness factor N_{-19}^{19} corresponds to the number of foreground SDSS galaxies with absolute magnitudes brighter than $M_r = -19$ within a 1.0 Mpc radius of the radio source. The foreground galaxy count is obtained by measuring the total number of sources in the $R=1.0$ Mpc disk and subtracting a background count, measured from a shell of inner and outer radii of 2.7 and 3.0 Mpc respectively. When SDSS data were unavailable (14% of the local sample), 2MASS K_s -band and EIS Patch-D I-band data were used. Finally, in cases where the apparent magnitude corresponding to $M_r = -19$ was fainter than the catalogue magnitude limit, a lower limit on N_{-19}^{19} including all sources within the disk and shell was used. According to Wing & Blanton (2011), a cluster-richness of $N_{-19}^{19} \leq 20$ likely corresponds to a poor cluster, while $N_{-19}^{19} \geq 40$ corresponds to a rich cluster. We thus decided to use $N_{-19}^{19} = 30$ to differentiate between poor and rich environments.

OTHER FACTORS

Several other factors might be in play, in particular properties of the host galaxies (Owen & Ledlow 1994) and polarisation (Banfield et al. 2012). We investigated both parameters by (1) including I-band absolute magnitudes, M_r , compiled from I-band data from either the SuperCosmos Sky Survey or the ESO Imaging Survey patch D and (2) retrieving polarisation data from NVSS.

HIGH/LOW EXCITATION GALAXIES

HEG/LEG classification was determined here by measuring the $[\text{OIII}]$ ($\lambda = 4959\text{\AA}$ and 5007\AA) and $[\text{OII}]$ ($\lambda = 3727\text{\AA}$) lines. We then followed the definitions of Jackson & Rawlings (1997): sources with OIII line width $< 1\text{nm}$ and/or $[\text{OII}]/[\text{OIII}] > 1$ were classified as LEG, other sources being classified as HEG. If no $[\text{OIII}]$ line was detected, the source must then be low excitation.

For the extended local sample, we found 81 LEG (49 FRI and 32 FR II) and 58 HEG (12 FRI and 46 FR II). The 44 other sources (14 FRI and 30 FR II) do not have spectra available to determine the excitation level of the host galaxy.

The local radio luminosity function was computed for both HEGs and LEGs. Sources with no HEG/LEG classification available were taken into account by including a correcting factor to each LRLF. The resulting LRLFs are shown in Figure 1.

We see that both HEGs and LEGs cover the full range of radio luminosities studied, and broadly agrees with the work of Best & Heckman (2012), indicating that the inclusion of sources with no HEG/LEG classification was properly done.

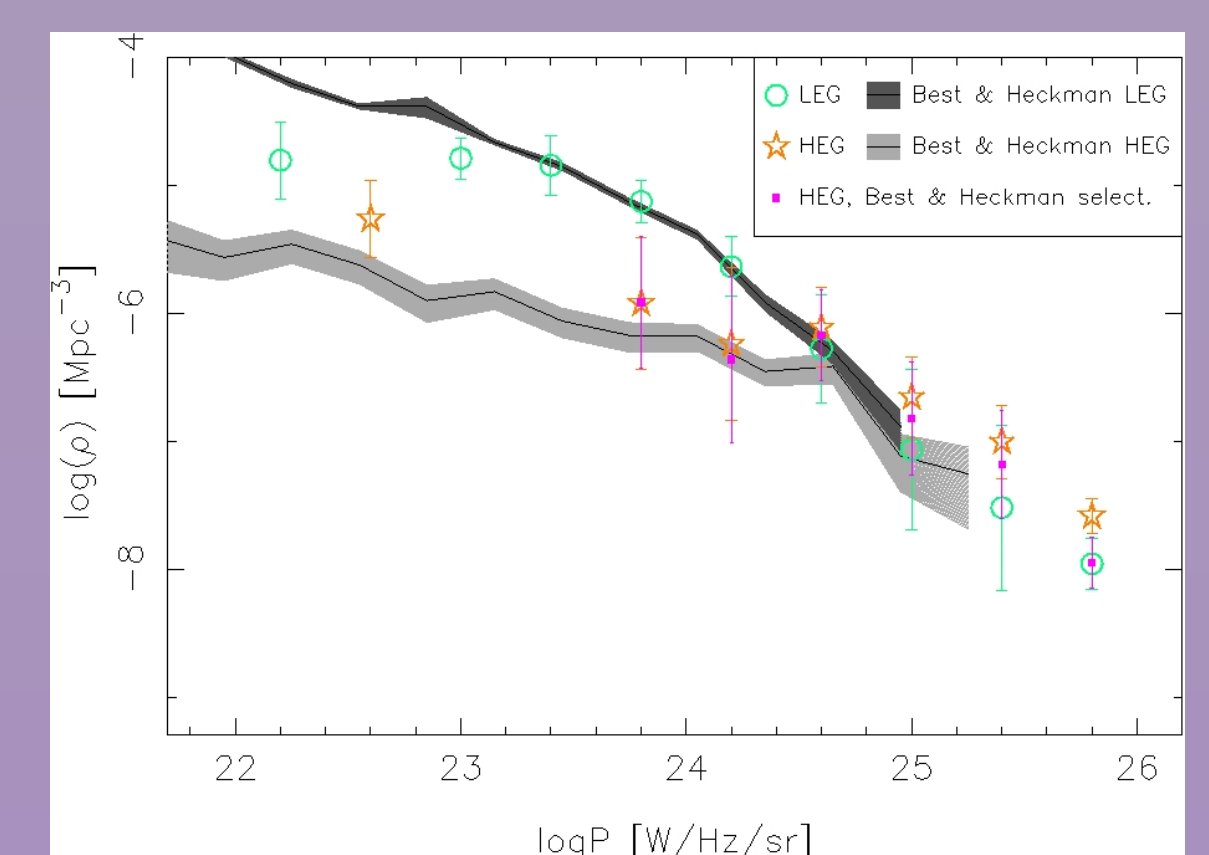


Figure 1: Local radio luminosity function for HEGs (orange stars) and LEGs (green circles) separately, using bin sizes of $\Delta \log P_{1.4\text{GHz}} = 0.4$. The LRLFs are compared to results from Best & Heckman (2012) in light and dark grey for HEGs and LEGs respectively. For more accurate comparisons, the LRLF for HEGs with SDSS counterparts (excluding QSOs) as selected by Best & Heckman (2012) is shown in pink filled squares.

RESULTS

From Figure 2, 3 & 4, we can see that:

- Both HEGs and LEGs give rise to radio sources of FR type I or II.
- Radio sources in rich clusters have a very high probability of being FRI (as previously stated by e.g. Prestage & Peacock 1988) and show low-excitation. The latter can be explained by the fact that jets in massive galaxies with low cooling-rates, giving rise to LEGs (Hardcastle et al. 2007), are easily disrupted, resulting in FRI-like morphologies in dense environments. On the other hand, HEG sources, both FRI and FR II, are found almost exclusively in low-density environments.
- The predominant population switches from FRI-LEGs to FR II-HEGs between low- and high-powers, with a break around $\log P \sim 24.6$ W/Hz/sr.
- While FRIs prevail at the low-luminosity LEG population, at $\log P \geq 23.8$ W/Hz/sr, LEGs seem to include similar fractions of FRI and FR IIs.
- Space-densities for FRI sources show similar shapes in all four categories. This implies that, for a given luminosity and excitation mode, there is no preferred environmental constraint to the source being of type-I morphology.
- FR IIs show an apparent switch from LEGs to HEGs with increasing power, with a divide at $\log P \sim 24.6$ W/Hz/sr. This is an indication that FR II morphology might be dependent on both the accretion mode and the luminosity of the AGN, on top of cluster environment.
- No major trends in the determination of FRI vs FR II are noticed in optical-vs-radio luminosity plots compiled for both low- and high-excitation galaxies. However, we can see that HEGs have more polarised sources than LEGs, and that low-density environment FR II have a very high probability to be polarised, whether they are a HEG or LEG.

Overall, we find that there is a broad overlap of properties, although FRIs generally reside in denser environments than FR IIs. In addition, a source found in a rich environment has a very high probability of being both LEG and FRI, fitting with scenarios in which cooling occurs from the X-ray halo. However, in most cases, the combined knowledge of a source's optical and radio luminosities, environment, excitation mode and polarisation will not allow for the morphological classification of the object. It seems that visual examination of the radio source is still the most reliable way of determining the FR type of an object.

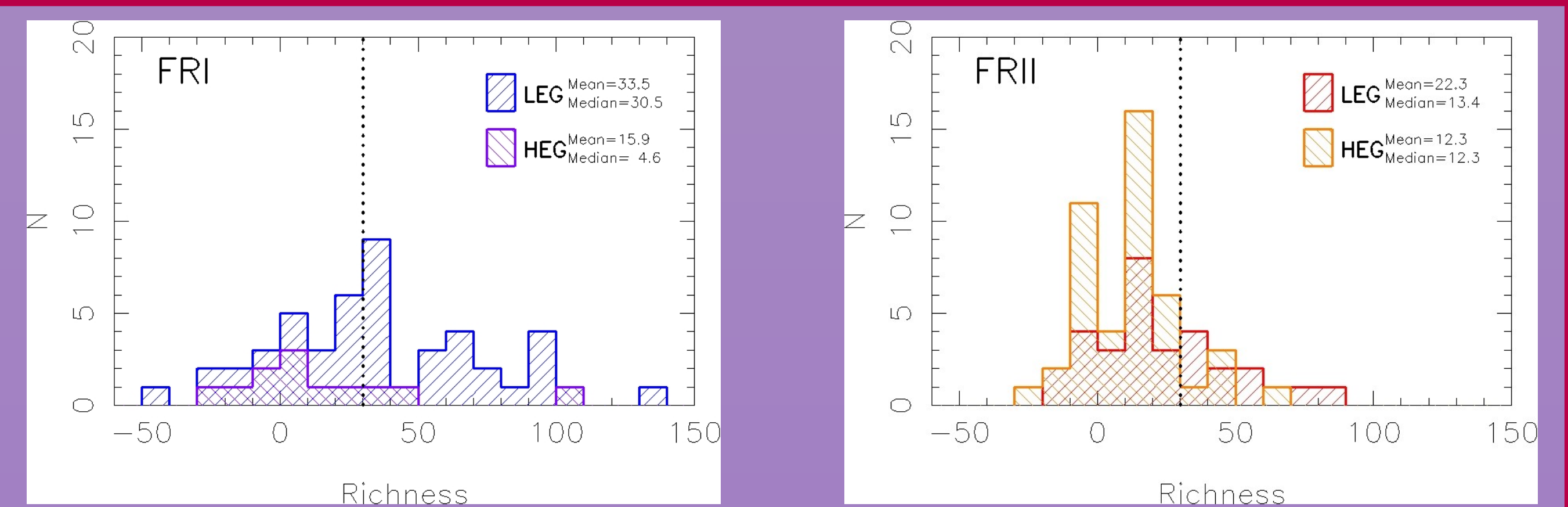


Figure 2: Distribution of sources as a function of richness factor N_{-19}^{19} , (including lower limits) for FRI (left) and FR II (right) sources. Each morphology group was additionally divided into LEG (upward slanted) & HEG (downward slanted) populations. Mean and median richness for each of the four groups are stated. The poor-to-rich division of $N_{-19}^{19} = 30$ is shown as a dotted line.

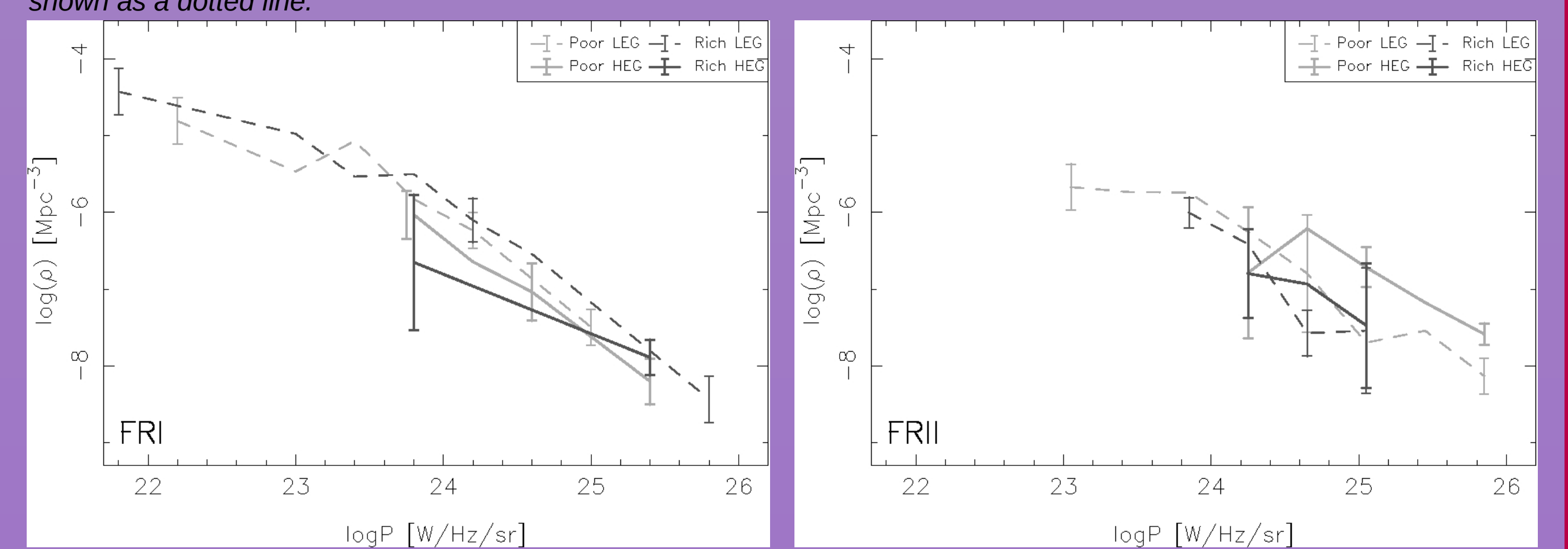


Figure 3: Local radio luminosity function $\rho(rho)$ for FRI (left) and FR II (right) sources, using bin sizes of $\Delta \log P_{1.4\text{GHz}} = 0.4$. Each morphology group was additionally divided into LEG (dashed lines) & HEG (solid lines) populations in poor (light grey) and rich (dark grey) environments (including lower limits).

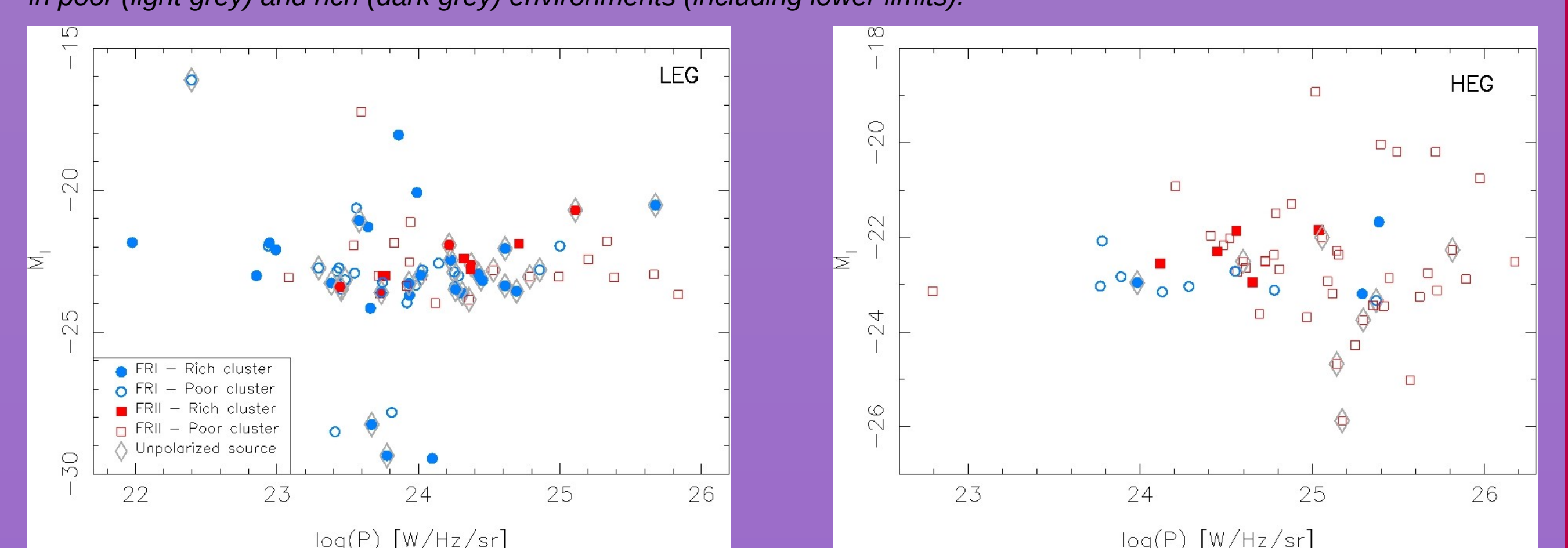


Figure 4: I-band vs. radio luminosity for LEG and HEG galaxies. Each population is divided between FRI (blue circles) and FR II (red square) in rich (filled symbols) and poor (open symbols) environments. Sources showing no polarised flux are outlined with light grey diamonds.